RMIB GERB Processing: Scene identification

Nicolas Clerbaux, Steven Dewitte

1st February 2002

MSG-RMIB-GE-TN-0007

Contents

CHANGE RECORD

Issue	Date	Approved by	Reason for change
Version 1	08/07/1999		new document
Version 1.1	29/09/99		CDR review

1 Introduction - Purpose of this document

The purpose of this document is to give a detailed overview of the scene identification process that will run at RMIB on the flow of Meteosat-7 or SEVIRI data. In the GERB RMIB ground segment, the scene identification is needed mainly to select adequate angular dependency model for radiances conversion into fluxes.

2 Generalities

2.1 Need of Scene Identification in the GERB Ground Segment

2.1.1 Choice of ADM for the Solar Reflected Radiation

Scene identification is needed in the GERB RMIB Ground Segment to select the adequate angular dependency model to convert the solar reflected unfiltered radiance L_{sol}^{uf} into solar reflected unfiltered flux F_{sol}^{uf} (see [AD8]).

For the thermal radiation, the flux inference from radiance does not need an explicit scene identification: the ADM choice is done by spectral analysis of the NB radiances of the imager ("implicit identification").

So, as the solar reflected radiance is obviously null during the night, the scene identification is needed only during day time for the ADM choice purpose.

2.1.2 Cloud flag derivation

An other use of scene identification is the derivation of cloud flag image corresponding to the GERB final product. The cloud flag information is known to be very important for the climatology community for derivation of averaged (e.g. monthly) clear sky albedo and clear sky thermal flux by removing data contaminated by cloud (see [De98]). For example, the widely-studied "cloud radiative forcing" is evaluated by comparison of clear sky values with total scene values (that means including the clouds).

Ideally, cloud flag images should be provided for all GERB level 2 products and then should be derived during the day and the night.

2.1.3 Should the Scene Identification be done during night?

To date, the planned scene identification system within the RMIB GERB processing is only run during day time and is based on the solar reflected NB radiances of the imager. This system could not provide cloud flag during night. So, cloud flag are no derived during night. A cloud detection algorithm based only on thermal radiances should be added in the future (TBD).

2.2 Minimal Set of Classes To Be Discriminated

The minimal set of classes to be discriminated depends on the set of available angular dependency models. For the ERB angular dependency models, the scene identification should at least discriminate between 12 classes (see [AD8]). For the "next century" ADM's (derived at Langley by the CERES team) approximately 200 models will be available. The scene identification detailed hereafter is designed to allow discrimination amon a large panel of different Earth-atmosphere scenes.

2.3 Scene Identification Overview

Figure 1 gives an rough overview of the scene identification system that is used within the GERB RMIB ground segment. This figure shows the 4 main subsystems of the scene identification system:

- conversion of NB radiance(s) into NB reflectance(s) (all slot)
- the clear sky reflectance images building process (weekly process)
- the surface identification (weekly process)
- the cloud analysis process (all slot)

These 4 subsystems are described in sections 3 to 6 hereafter.

The scene identification generates two kinds of products :

- the surface related products which are produced on a regular basis (to date weekly) and,
- the cloud related products which are produced for each imager slot (15' for SEVIRI and 30' for MS-7).

2.4 Imager Characteristics

2.4.1 Introduction

Two imaging systems may be used in the GERB Ground Segment: the imager on-board Meteosat-7 satellite and the SEVIRI imager on-board the future MSG-1 satellite. The Meteosat-7 imager is operational since June 1998 and is planned to remain operational at least until SEVIRI is fully operational. This imager is important for the development of the GERB ground segment at RMIB because it is planned to be used during the SEVIRI commissioning phase.

2.4.2 Meteosat-7 imager

Like the others imagers of the Meteosat serie, the imager on-board the Meteosat-7 satellite has 3 spectral channels:

- a visible band channel (radiance L_{vis}),
- a water-vapor channel (radiance L_{wv}),
- a infrared channel (radiance L_{ir}).

Only one channel is available in the solar part of the spectrum. Nevertheless, the infrared channel may probably be used to discriminate cloud according to their phase (water droplets or ice particles) (TBC).

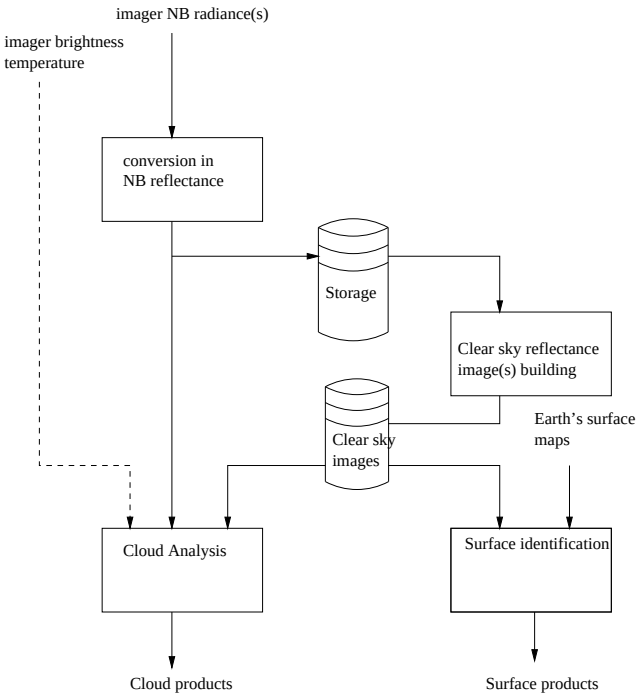

Figure 1: Overview of the RMIB scene identification system. The inputs are the NB radiances of an imaging device (e.g. SEVIRI). The system generates two kinds of products: the surface products (to date weekly) and the cloud product (for each imager slot).

channel name	type	#filter	μ_i	σ_i	lower (1%)	upper (99%)
HRV	BB visible	0				
VIS 0.6	visible "green"	1	0.635 μ	0.025μ	0.56μ	0.71μ
VIS 0.8	visible "red"	2	0.81μ	0.030μ	0.74μ	0.88μ
IR 1.6	NIR water/ice	3	1.64μ	0.061μ	1.50μ	1.78μ
IR 3.9	window	4	3.92μ	0.191μ	3.48μ	4.36μ
IR 6.2	water vapor	5	6.25μ	0.301μ	5.35μ	7.15μ
IR 7.3	water vapor	6	7.35μ	0.217μ	6.85μ	7.85μ
IR8.7	window	7	8.70μ	0.174μ	8.30μ	9.10μ
IR9.7	O_3	8	9.66μ	0.122μ	9.38μ	9.94μ
IR 10.8	window	9	10.8μ	0.435μ	9.8μ	11.8μ
IR12	window	10	12.0μ	0.435μ	11.0μ	13.0μ
IR 13.4	CO_2	11	13.4μ	0.435μ	12.4μ	14.4μ

Table 1: The 12 SEVIRI channels. The table gives for each channel: EUMETSAT names, type of channel, channel index (internal at RMIB), mean and standard deviation when spectral filters are modeled with Gaussian shape, expected lower and upper limits

2.4.3 SEVIRI imager

The future MSG imager, SEVIRI, has 12 spectral channels designed for meteorological applications. The table 1 gives the expected characteristics of these channels. This information is available from the SEVIRI Science Plan [SSP].

The HRV (High Resolution Visible) channel has neither the same spatial resolution nor the same coverage of the Earth's disk than the others channels. For this reason the HRV radiances will not be used for scene identification.

The $IR3.8\mu$ channel lies at the cut-off between short wave and long wave radiation and is then sensible for both the solar reflected energy L_{sol} and thermally emitted energy L_{th}. For this reason, this channel is not used for scene identification.

These two channels removed, scene identification takes as input 3 NB channels in the short wave part of the spectrum: the $VIS\,0.6\mu$, $VIS\,0.8\mu$ and $IR\,1.6\mu$.

3 Converting NB Radiance into NB Reflectance

3.1 Introduction, Reflectance Definition

The NB radiances L_i measured by an imager are not good features to characterize a scene. Indeed, for a given scene, the measured radiances is strongly dependent on the illumination and vary then with the solar zenith angle θ_s and with the Earth-sun distance d.

Narrow-band reflectances ρ_i are more interesting features to characterize a scene:

$$\rho_i = \frac{L_i}{\cos\theta_s \frac{1}{d^2} L_i^{solspec}} \tag{1}$$

where

- d is the Earth-sun distance expressed relatively to the mean Earth-sun distance,
- $L_i^{solspec} = \int_0^\infty L(\lambda)\,\phi_i(\lambda)\,d\lambda$ is the solar radiance caught by the spectral response curve $\phi_i(\lambda)$ of the i^{th} channel of the imager.

The reflectances ρ_i are dimensionless and can be interpreted as kinds of "spectral albedo for lambertian scene". Obviously, for a given scene, the reflectances ρ_i measured at the satellite do not remain constant during the sun motion because of the bidirectional behavior of the scene.

3.2 Implementation

For each imager channel, the conversion 1 is realized by a simple program ('rad2ref') that takes as input:

- the image of radiance L_i (floating point image),
- the image of solar zenith angle θ_s for the current slot (floating point image),
- the solar radiance caught by the imager channel spectral response curve $L_i^{solspec}$ (scalar value) and,
- the Earth-sun distance d (scalar value updated for each slot).

The program generates a floating point image that contains, for each pixel of the imager FOV, the reflectance value ρ_i for this channel.

4 Clear Sky Reflectances Images

4.1 Introduction

Clear sky images are defined as the images that should be seen (or derived) by the imager is none of the pixels is contaminated by cloud. Within the SEVIRI scene identification part of the GERB RMIB Ground Segment, clear sky reflectance images are derived to fulfill 2 goals:

- to serve as basic inputs for the surface identification process (see section §5)
- to serve as input for the cloud analysis product (see section §6). For a cloudy pixel ($\rho > \rho_{cs}$), an accurate estimate of the cloud optical thickness τ should take into account the value of the surface reflectance. That means reflectance under clear sky condition ρ_{cs}.

These clear sky reflectance images are updated on a regular basis. To date, a weekly update is used at RMIB.

4.2 Statistical Analysis of Reflectance

Lets $\{\rho_t\}$ be a temporal sequence of daily reflectance for a given pixel and a given imager slot of the day. The clear sky reflectance for this pixel for this slot of the day can be estimated by statistical analysis of the $\{\rho_t\}$ values. A simple and robust estimator of the clear sky reflectance ρ_{cs} is the quantile q of the $\{\rho_t\}$ distribution:

$$\rho_{cs} = Q_q(\{\rho_t\})$$

In practice, a quantile value between $q = 5\%$ and $q = 10\%$ has shown to give good result when the input temporal sequence extents on a period between 30 and 60 days.

4.3 Building Clear Sky Reflectance

4.3.1 Reflectance Images Storage

To compute clear sky reflectance by the quantile method explain before, the last reflectance images must be stored on hard disk for a set of slots during the day. Lets C be the number of short wave channels of the imager, S be the number of slot of the day for which clear sky are computed, N be the storage period in days. The number of reflectances images that are stored is then the product :

$$C * S * N$$

Typical values for these factors are :

- $C = 3$ (the 3 solar channels of SEVIRI),
- $S = 14$ (one slot per hour from 6 a.m. to 19 p.m.),
- $N = 60$ (storage extents on 2 months)

This leads to a number of about 2500 stored reflectance images.

4.3.2 Implementation

The clear sky images are built using the RMIB program 'clearsky'. Inputs are :

- the path to the storage directory
- the quantile value (e.g. $q = 5\%$)
- the minimal number of reflectance values to compute clear sky reflectance (for example 30)

Outputs are the floating point clear sky reflectances images for the various slot of the day.

4.3.3 Results

Clear sky reflectance image at 12 h for the visible band of MS-7 is shown on figure 2.

4.4 Shortcomings

4.4.1 Residual cloud

Residual clouds can be observed in some areas mainly near the wintertime pole.

4.4.2 Cloud shadows

Cloud shadows may be observed at dawn and dusk above high reflectivity areas such as deserts. The figure 3 shows the clear sky reflectance for MS-7 visible band at 8 a.m. over North Africa.

4.4.3 Vegetation onset

To be investigated.

4.4.4 Snow fall and melting

The fresh snow does not appear on clear sky images because of the inertia of the building process. The fresh snow is treated as a part of the 'cloud product'.

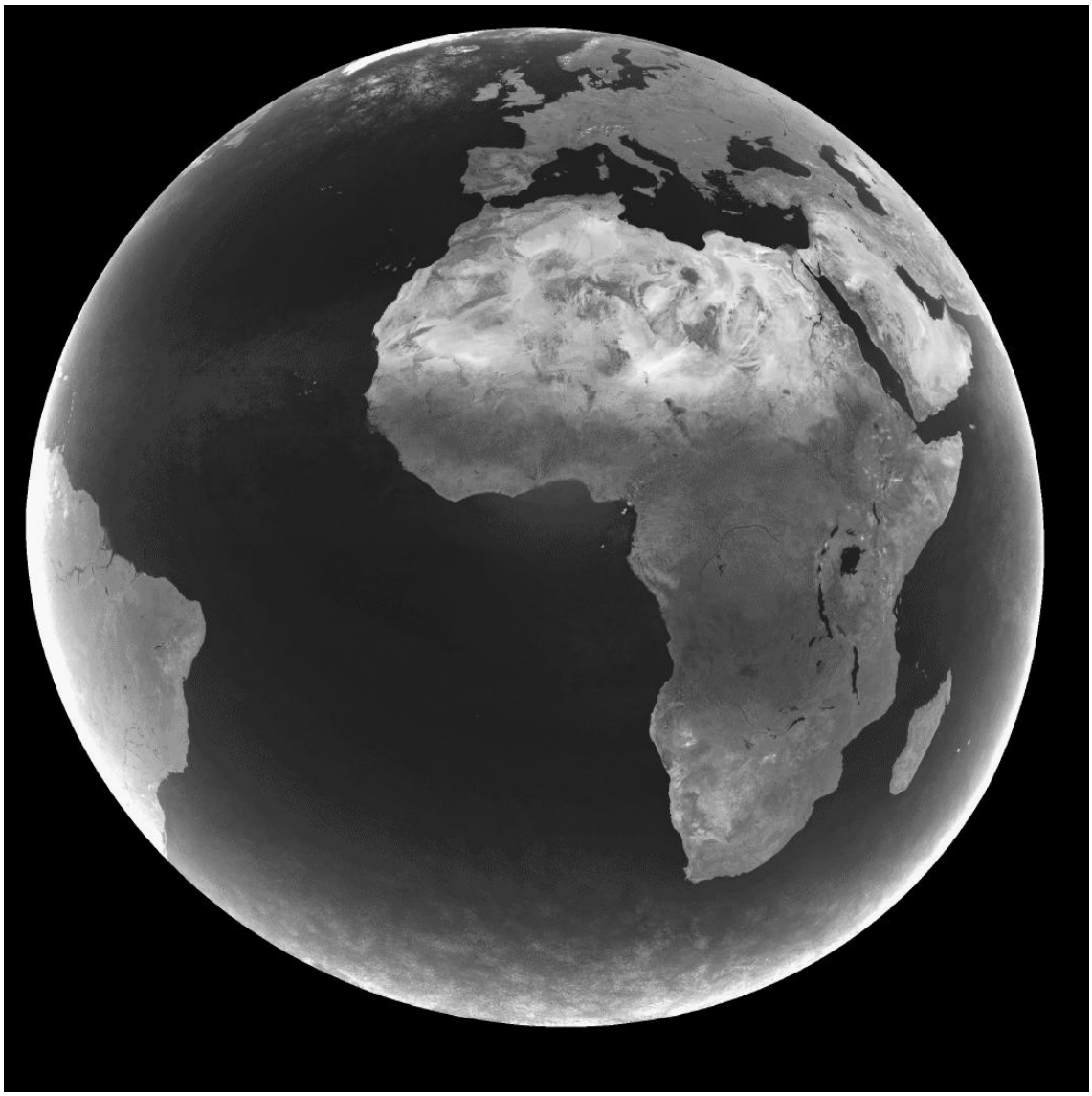

Figure 2: Clear sky reflectance image for the 12h Meteosat-7 visible band slot (July-August 1999). Brightness extents from $\rho = 0$ to $\rho = 0.4$.

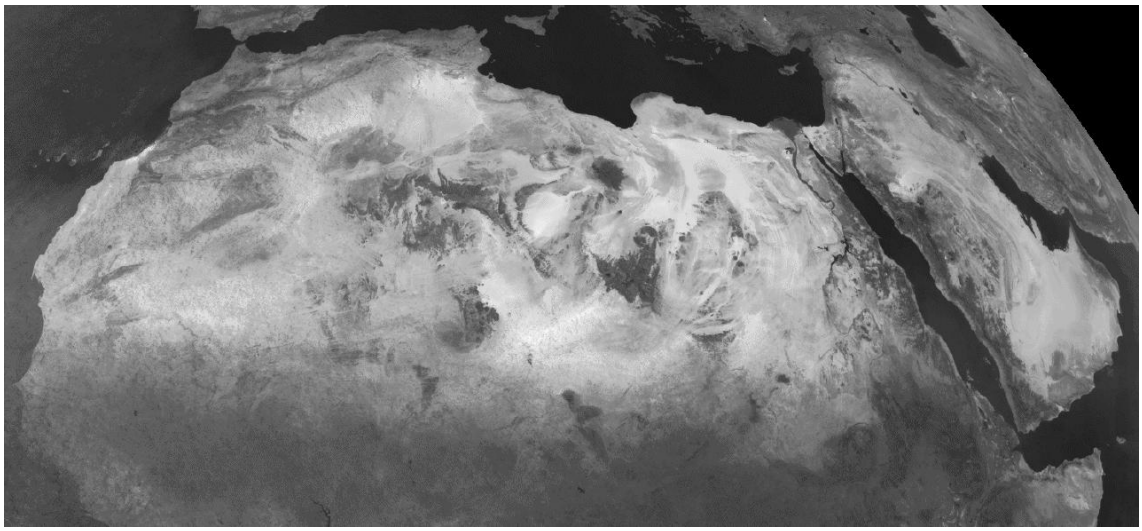

Figure 3: Clear sky reflectance image at dawn over North Africa for the Meteosat-7 visible band slot. The desert 'texture' is due to cloud shadowing and local orography. Brightness extents from $\rho = 0$ to $\rho = 0.4$.

4.5 Temporal Interpolation of Clear Sky Reflectance

4.5.1 Goals

To limit the disk space needed for reflectance images storage, these images are stored only for one slot per hour. As the imager generates images at higher rate (2 per hour for MS-7 and 4 per hour for SEVIRI), temporal interpolation on the clear sky reflectance images must be done.

4.5.2 Implementation

The RMIB program 'cs_interpolation' performs the linear temporal interpolation between 2 clear sky reflectance images to product clear sky reflectance image for an intermediate time. Using this program, it is possible to generate a clear sky images for each imager slot.

4.6 Overview

The figure 4 shows the two main steps to build the clear sky reflectance images within the RMIB SEVIRI processing : (i) first, clear sky image building for one slot per hour and all imager channels and (ii) secondly interpolation between these images to get clear sky images for all slots and all channels.

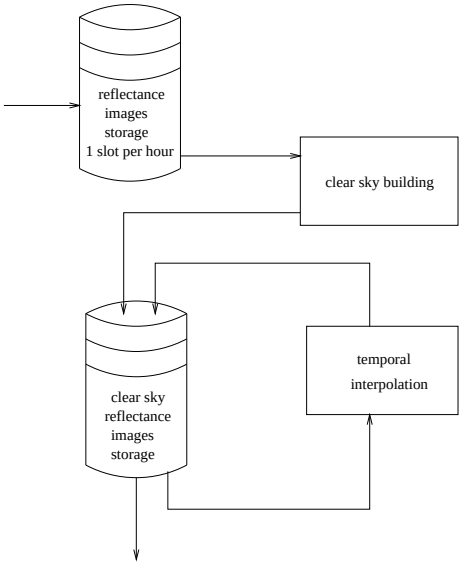

Figure 4: Overview of the clear sky reflectance images building with its 2 subprocesses: the clear sky computation for 1 slot per hour and the temporal interpolation between these slots to get clear sky images for all the imager slots.

5 Surface Identification

5.1 Goals

The surface identification subsystem aims to feature and class the imager pixels according to the Earth's surface angular behavior. The classification should discriminate at least the minimal set of surface classes :

- ocean (and all other water surface types: lake, river, ...),
- land,
- desert,
- snow (including ice sheet, ...).

As for the clear sky image building, the surface identification can be done on a regular basis such as a weekly update. The basic input for the surface identification are the clear sky NB reflectance images. The following information can be extracted from these images :

- surface broadband reflectance,
- surface spectral characteristics when the imaging system provides various measurements in the short wave region (it is the case of SEVIRI but not of MS-7),

- surface angular behavior by analysis of the (clear sky) broadband reflectance variation during the day.

To extract more easily these informations, the NB reflectance image(s) are transformed into broadband reflectance image and eventually (in case of multispectral imager) spectral feature images as explained in the next section.

5.2 Narrow-band Reflectance Images Transformation

5.2.1 Meteosat-7 case

As there is only one channel in the solar reflected region, it is not possible to derive spectral feature images. The visible band reflectance image are converted into broadband reflectance image by:

$$\rho_{BB} = 0.0407 + 0.7411\,\rho_{vis} \tag{2}$$

where the unfiltering formula 2 is independent of the scene.

5.2.2 SEVIRI case

The reflectances at 0.6μ, 0.8μ and 1.6μ are converted into the broadband reflectance ρ_{BB} and 2 spectral coefficients: $NDVI$[1] and $\rho_{1.6\mu}$.

$$\begin{gathered} \rho_{BB} = 0.047 + 0.3708\,\rho_{0.6} + 0.3567\,\rho_{0.8\mu} \\ NDVI = \frac{\rho_{0.8\mu} - \rho_{0.6\mu}}{\rho_{0.8\mu} + \rho_{0.6\mu}} \\ \rho_{1.6\mu} = \rho_{1.6\mu} \end{gathered} \tag{3}$$

5.2.3 Note

The regression laws to infer the BB reflectance ρ_{BB} from the imager NB reflectances ρ_i are obtained using the same methodology as the one used in the spectral modeling part of the SEVIRI processing (for more details see the spectral modeling document [AD5]).

5.2.4 Implementation

The image of BB reflectance ρ_{BB} is obtained from the images of NB reflectance using the 'im_regression' program. This program is widely used in the frame of spectral modeling. The $NDVI$ image is computed from the images of NB reflectances using the RMIB program 'ndvi'.

[1] $NDVI$ = is the Normalized Difference Vegetation Index and is widely used to characterize the kind of land surface and vegetation.

5.3 Local Noon Images

5.3.1 Goal

To reduce the importance of Rayleigh scattering in the atmosphere, local noon images are computed from the clear sky images. Local noon image is built by interpolating diurnal sequence of images to extract value when the solar zenith angle θ_s is minimal. At local noon, the optical path within the atmosphere is minimal, the surface illumination is maximal and then the signal caught by the sensor is maximal.

Local noon images are built for :

- the imager NB reflectance $\rho_{0.6\mu}$, $\rho_{0.8\mu}$ and $\rho_{1.6\mu}$ (SEVIRI) or ρ_{vis} (Meteosat-7),
- the broadband reflectance ρ_{BB} obtained from NB reflectance by 2 or 3,
- the $NDVI$ and the $\rho_{1.6\mu}$ spectral feature images (SEVIRI only).

5.3.2 Results

Figure 5 shows the local noon clear sky reflectance image ρ_{vis} for July-August 1999 derived from the MS-7 visible band channel. Comparison with figure 2 shows clearly the reduction of the Rayleigh scattering on local noon image.

5.3.3 Implementation

The RMIB program 'local_noon' computes the local noon image by analysis and interpolation within of a sequence of images. This program serves to compute local noon images for the NB clear sky reflectance images and for the clear sky BB reflectance images ρ_{BB} and the spectral feature images ($NDVI$ and $\rho_{1.6\mu}$).

This program can also be used to build the images of viewing angles $\{\theta_{v,}\theta_{s,}\phi)$ corresponding to the local noon images.

5.4 Characterizing the Bidirectional Reflection Behavior

5.4.1 Introduction

For each pixel in the imager FOV, it is possible to extract from the diurnal serie of clear sky BB reflectance images a curve of the variation of this quantity during the sun motion. This curve is representative of the bidirectional behavior of the surface and can be compared to the standard curves that are known for the ERB classes.

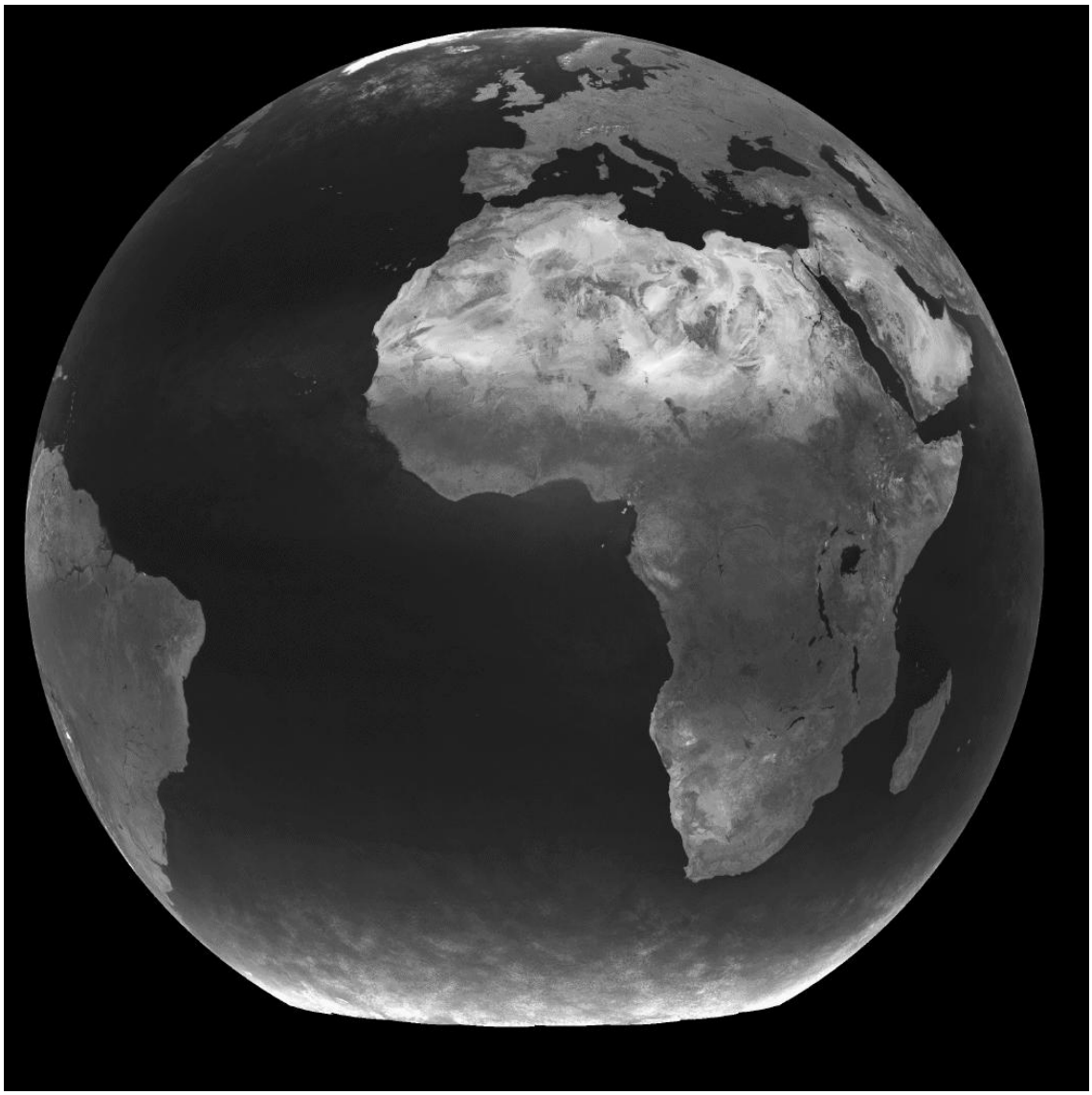

Figure 5: Local noon clear sky reflectance image for MS-7 visible band channel during summer in the Northern hemisphere. Brightness extends from $\rho = 0$ to $\rho = 0.4$.

5.4.2 Distance to ERB classes

For each ERB class, it is possible to build the broadband reflectance curve as :

$$\rho_c = A_c(\theta_s)\, R_c(\theta_s, \theta_v \phi)$$

where

- $A_c(\theta_s)$ is the albedo for the ERB class c for the solar zenith angle θ_s
- $R_c(\theta_s, \theta_v, \phi)$ is the bidirectional reflectance for the ERB class c and the viewing angles $(\theta_s, \theta_v, \phi)$

The distance in the sense of bidirectional reflectance is defined as the best match of the curves ρ_{BB} and ρ_c :

$$d_c = MIN_\alpha(\|\rho_{BB} - \alpha\, \rho_c\|) \tag{4}$$

where the minimization on the scaling factor α is done to take into account difference of surface albedo and $\|\|$ is the L_2 distance.

5.4.3 Shortcomings

1. The first and main shortcoming of the distance 4 for classification is that in some part of the imager FOV, the Sun-Earth-Satellite configuration $(\theta_s, \theta_v, \phi)$ is "undiscriminant" in the sense of bidirectional reflection. For example, but it is not the sole case, at high viewing and solar zenith angles the Rayleigh scattering does the bidirectional reflectance be the close for all the classes (in this situation $R_c(\theta_s, \theta_v, \phi)$ becomes the bidirectional reflectance of the atmosphere instead of the one of the surface).
2. high quality bidirectional reflectance models must be available,
3. The computing of the distance d_c is heavy and time expensive because for all imager pixel: (i) reflectance curve ρ_{BB} and the ERB curves ρ_c for must be built and (ii) the optimization 4 must be done for all classes.

5.4.4 Implementation

The RMIB program 'erb_distance' computes, for each pixel of the imager FOV, the distances d_c to the 4 clear sky ERB classes (ocean, land, snow and desert). The program inputs are :

- the serie of BB reflectance images ρ_{BB},
- the serie of viewing angles images,
- the albedo A_c and BRDF R_c for the ERB classes.

This program generates 4 images (one for each ERB class) of the distance to ERB classes $\{d_c\}$.

5.5 Classification

5.5.1 Introduction

For each pixel within the sensor FOV, the following features are available:

- the broadband reflectance ρ_{BB} at local noon,
- the spectral features $NDVI$ and $\rho_{1.6\mu}$ (SEVIRI only),
- the angular behavior by means of the distance to ERB classes $\{d_c\}$.

These scalar values form the feature vector:

$$\overrightarrow{f} = \{\rho_{BB}, NDVI, \rho_{1.6\mu}, d_c\} \tag{5}$$

.

From these features, classification consists to assign at the pixel a label corresponding to the closest kind of surface within a predefined set. To date, the classification only discriminates 4 classes: ocean, land, desert and snow. In the future, this set may probably grows for example by splitting some class into subclasses (ice sheet/fresh snow, open ocean/ coastal ocean, ...) according to the set of bidirectional models that will be available to convert radiance into flux.

5.5.2 Classification methods

Classification is done on a supervised approach. That means that data sets of feature vectors 5 are built for the various kinds of surface that have to be discriminated. Then supervised classification methods (e.g. standard Gaussian classifier or neural networks) have shown to discriminate easily between the main kinds of surface.

5.5.3 Validations

Classification was been validated by 2 ways at RMIB:

1. using Meteosat-7 images, the classification based on broadband reflectance and angular behavior was implemented and was proved to discriminate the 4 ERB classes.
2. using ATSR-2 (on ERS-2 satellite) data, the classification based on broadband reflectance and spectral features was tested. This instrument has 3 spectral channels in the solar reflected region which are close to the SEVIRI channels. It was shown that these features are very informative to discriminate between ERB classes. The figure 6 shows the distribution of the {ocean, land, snow, desert} classes in the three-dimensional reflectance space of ATSR-2.

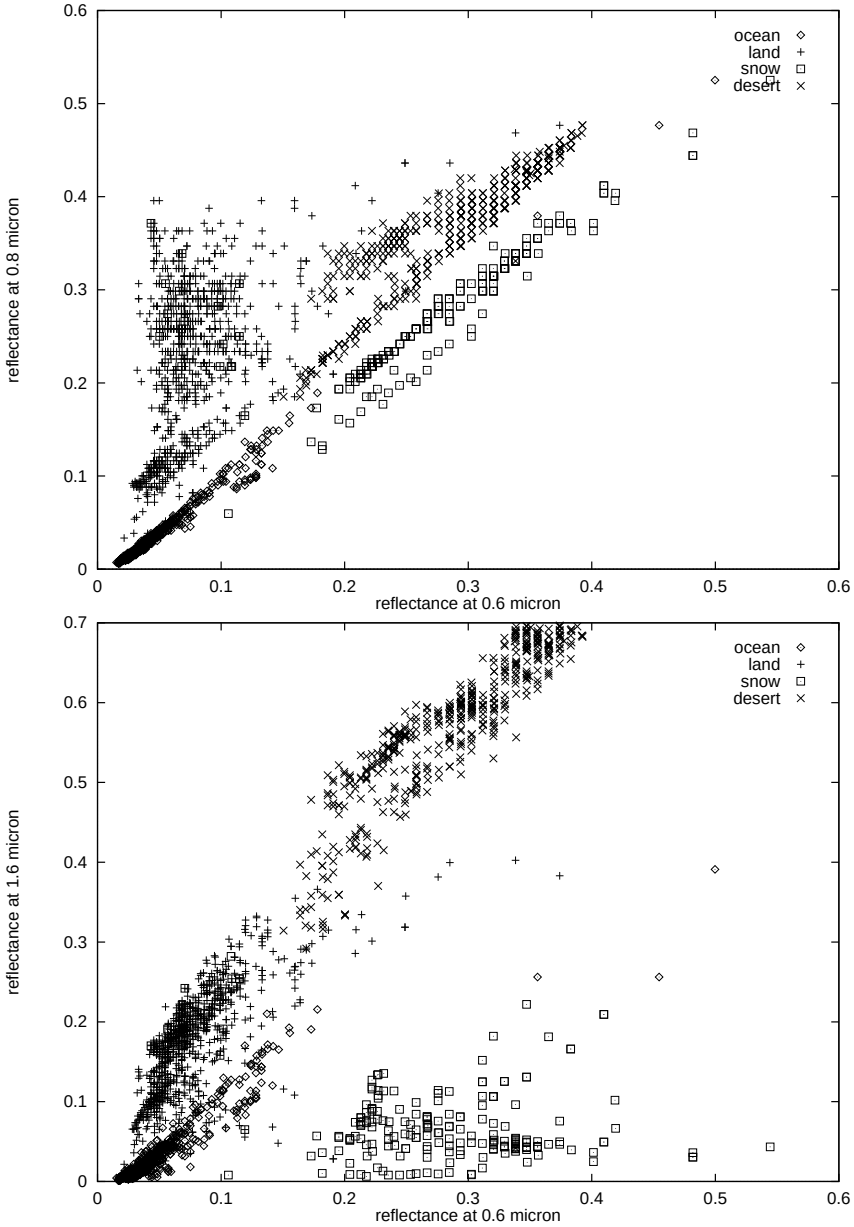

Figure 6: Distribution of the 4 ERB classes {ocean, land, snow, desert} in the reflectance space $\{\rho_{0.6\mu}, \rho_{0.8\mu}, \rho_{1.6\mu}\}$ of the ATSR-2 instrument. On the upper figure, a high correlation appears between the 0.6μ and 0.8μ channels excepted for land surfaces due to $NDVI$ effect. The lower figure shows a good classes separation in the $\{\rho_{0.6\mu}, \rho_{1.6\mu}\}$ sub-space. In particular, the 1.6μ channel allows a good discrimination between snow and other high reflective surface (desert).

5.5.4 Shortcoming

Some classification problem may occur in sun glint area (TBC) and at high viewing zenith angles θ_v due to Rayleigh scattering. To solve the sun glint problem, the local noon program may be modified in order to extract values for the higher sun elevation above the horizon but only when tilt angle[2] is higher than a threshold of 25^o (TBD/TBC).

5.5.5 Implementation

Feature data sets building A first program ('pixel_encoding') allows user to build easily dataset of feature vectors $\overrightarrow{f}$ for the various kinds of classes one wants to discriminate. A false color image of the clear sky local noon NB reflectances (combining the local noon NB reflectance images blue=$\rho_{0.65\mu}$, green=$\rho_{0.85\mu}$ and red=$\rho_{1.6\mu}$) is visualized on a workstation. Then, for each class to be discriminated, user has to indicate (with the computer mouse) a set of pixels that belong to the class.

Classification tuning The classification programs ('Classif') takes as input these data sets of feature vectors and gives various methods for supervised classification (neural network, Gaussian classifier, nearest neighbor, ...).

Classification itself The RMIB program 'im_classif' takes as input the various images of feature and some parameters generated by the classification tuning (weights of the neural network, ...). For each pixel in the FOV, classification is performed. The program generates an image of surface label.

In case of failure (one or multiple features not available) an undefined class is assigned to the pixel.

5.6 Heuristics

5.6.1 Goal

Maps of the Earth's surface occupation are used in the RMIB Scene Identification subsystem to help surface identification when identification is hazardous. For example :

- for areas where the clear sky values can not be derived or
- for areas with high viewing zenith angles ($\theta_v > 80^o$) where the Rayleigh scattering screen off the surface properties.

[2]The tilt angle is the angle between the direction of specular solar reflection and the satellite line of sight.

5.6.2 Implementation

The Earth's surface map are transformed to correspond to the imager geolocation table. Then the program RMIB 'heuristic' fills the undefined values in the label image.

5.7 Lower Resolution Products

This surface identification explained before is done at the full imager resolution. As the final products that serve for the choice of ADM are done at lower resolution, the resolution of the label image is reduced using the 'im_class_reduce' program. During the resolution reduction process, additional classes may appear such as: 'mix ocean-land', ...

5.8 Conclusions

Surface identification is based on clear sky NB reflectance images. From these images, 3 kinds of information are extracted: the broadband reflectance ρ_{BB} at local noon, the spectral features ($NDVI$ and $\rho_{1.6\mu}$) at local noon and the angular behavior $\{d_c\}$.

At this time, with Meteosat-7, the broadband reflectance at local noon and the angular behavior is used as basic input for classification. This approach is heavy and does not lead to perfect results (the heuristic maps are often used).

For SEVIRI, it is explained that the addition of spectral features will improve noticeably the performances of the scene classification system. Heuristic maps will be used only where feature extraction can not be done. With SEVIRI, the additional $NDVI$ image at local noon is generated by the surface identification process. This image can be used to select appropriated BRDF model when angular models are derived for various land surface. The CERES team plans to derive BRDF for various land surface classified according to NDVI.

The figure hereafter summarizes the surface identification process.

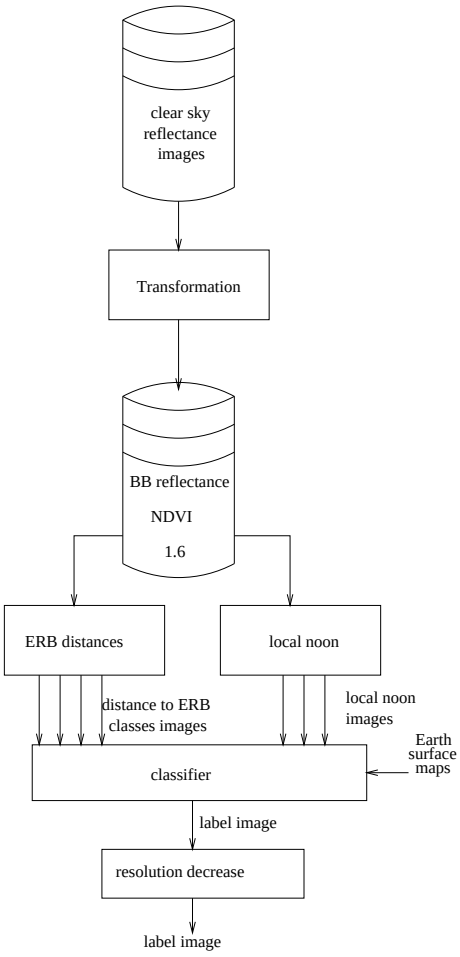

Figure 7: Overview of the surface identification subprocess within the RMIB scene identification process. The inputs for this subprocess are the clear sky reflectance images of the imager (Meteosat-7 or SEVIRI). The subprocess generates an image that contains for each pixel the kind of surface.

6 Cloud Analysis

6.1 Introduction

The cloud cover that may exist over the Earth surface is known to have strong influence on the bidirectional reflection behavior of the Earth-atmosphere system. The cloud analysis subsystem within the scene identification system aims to deliver a good parametrization of the cloud cover in order to select appropriated BRDF model in the radiance to flux conversion (see [AD8]). The cloud analysis must be done at the imager resolution (or the final product resolution) and at the imager slot rate.

6.2 MPEF Cloud Analysis Products

EUMETSAT MPEF will deliver a very complete cloud product known as *CLA* (as Cloud Analysis). This product will contain: cloud phase, cloud type, optical thickness, cloud top temperature and cloud top height (see the SEVIRI Science Plan [SSP]). In a second product, these informations will be provided according to 3 cloud layers (low, mid-altitude and high cloud).

To date, it is not planned to use MPEF products within the real time GERB RMIB processing because :

- this product is not yet fully defined and described,
- it is not yet known when do these products be available.

Nevertheless, EUMETSAT cloud products may be used in the future in the frame of real time processing or for GERB data reanalysis.

6.3 Cloud Optical Thickness τ

6.3.1 Introduction

The cloud optical thickness τ is usually derived from one of the visible channel(s) of an imaging system. Let ρ be the reflectance in this channel. To take into account the surface reflectance, the cloud optical thickness τ is estimated by comparison of three reflectance values for this channel:

- the measured NB reflectance ρ,
- the corresponding clear sky reflectance ρ_{cs},
- the modeled reflectance of an overcast scene ρ_{over} .

According to these values, a mean effective cloud cover C is derived as (see [SR91]):

$$C = \frac{\rho - \rho_{cs}}{\rho_{over} - \rho_{cs}} \tag{6}$$

and the cloud optical thickness τ is related to the mean effective cloud cover C by a single and constant relation (see [Jo99]):

$$\tau = \tau(C)$$

6.3.2 Modeling the Overcast Reflectance ρ_{over}

ERB overcast scene From the ERB classes (see [ERB]), the overcast reflectance may be estimated by:

$$\rho_{over}(\theta_s, \theta_v, \phi) \; = \; \alpha \, A_{over}(\theta_s) \, R_{over}(\theta_s, \theta_v, \phi) \tag{7}$$

where α is a spectral parameter that is added to convert the ERB broadband reflectance into reflectance for the selected visible band channel. This approach gives a good bidirectional behavior for the overcast scene but underestimate the overcast albedo. This is due to the not adapted definition of the overcast scene for the ERB model[3].

Using radiative transfer model Using a plane parallel radiative transfer code ([SBDART]) with an overcast cloud layer ($\tau = 300$), the spectral radiance

$$L(\lambda, \theta_s, \theta_v, \phi)$$

are computed for wavelength step of $d\lambda = 0.01\mu$, zenith angle step of $d\theta_s = d\theta_v = 5^o$ and relative azimuth step of $d\phi = 10^o$. The overcast scene reflectance model is built by spectral integration of the spectral radiance:

$$\rho_{over}(\theta_s, \theta_v, \phi) = \frac{\int_{0.25\mu}^{2.5\mu} L(\lambda, \theta_s, \theta_v, \phi) \, \phi(\lambda) \, d\lambda}{\cos\theta_s \int_{0.25\mu}^{2.5\mu} L^{solspec}(\lambda) \, \phi(\lambda) \, d\lambda} \tag{8}$$

where $L^{solspec}(\lambda)$ is the solar spectral radiance curve and $\phi(\lambda)$ is the spectral response curve of the visible band channel that serves for the optical thickness estimation.

The angular behavior in the model 8 has proved to be in good accordance with the ERB model 7. The overcast albedo in 8 is sensibly higher and closer to the reality than in the ERB model 7 (due to difference of definition of ERB overcast scene).

[3]For the ERB models, the overcast scene is defined as scenes totally filled by cloud, independently of the cloud optical thickness.

6.3.3 Meteosat-7 case

The reflectances in the imager visible band are used to estimate the mean effective cloud cover C and the cloud optical thickness τ.

Figure 8 shows the effective mean cloud cover image from the Meteosat-7 imager.

6.3.4 SEVIRI case

Two SEVIRI spectral channel may be used to estimate the cloud optical thickness : the 0.6μ channel or the 0.8μ channel. To reduce Rayleigh and aerosol scattering, the 0.8μ channel is often preferred to the 0.6μ channel over the sea. Over land surface, the 0.6μ channel is preferred (see [Jo99]). The mean effective cloud cover C and the cloud optical thickness τ are estimated using the 0.6μ or the 0.8μ channel with respect to the kind of surface (ocean/other) given by the surface identification subsystem.

To reduce propagation of sensor noise, an averaged reflectance may also be used (TBC):

$$\rho_{sev} = \frac{\rho_{0.6\mu} + \rho_{0.8\mu}}{2}$$

6.3.5 Validation

The validation of the NB reflectances for an overcast scene derived radiative transfer model $\rho_{over}(\theta_s, \theta_v, \phi)$ has been tested for the Meteosat-7 visible band channel. This model should also be validated for the SEVIRI channel using the ATSR-2 data (TBD).

The mean effective cloud cover 6 is validated using Meteosat-7 images.

6.4 Cloud flag

A cloud flag product is generated by thresholding the cloud optical thickness. The cloud flag is set up for pixel with :

$$\tau > \tau_{th}$$

with threshold value of about $\tau = 0.1$.

6.5 Cloud phase

6.5.1 Introduction

The cloud phase (water droplets or ice particles) could be derivate from NB measurements in absorption bands of ice particles (see [De99]). To date, most of the Earth Observing System includes a 1.6μ or 2.2μ channel to discriminate clouds according to their phase.

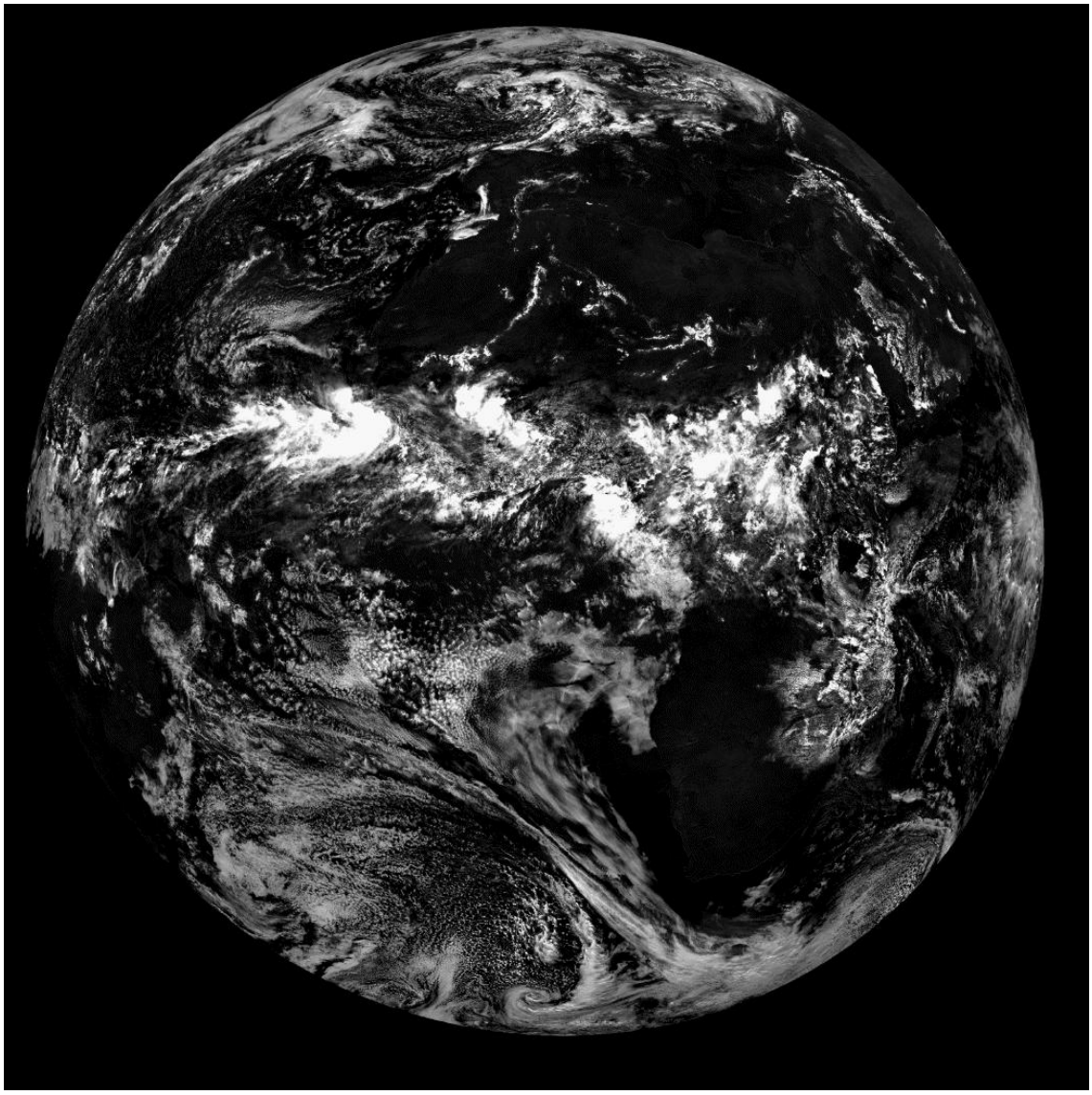

Figure 8: Image of effective mean cloud cover C (formula 6) from the Meteosat-7 imager for 16^{th} August 1999 at noon. Brightness extents from $C = 0$ to $C = 1$.

Without channel in the ice absorption bands, the brightness temperature measured in a thermal atmospheric window can be used as estimator of the cloud top temperature and then indirectly to the cloud top phase.

6.5.2 Meteosat-7 case

Using only the visible channel of MS-7, the cloud phase determination is known to be nearly impossible. So, the brightness temperature determinated from the imager window channel $T_{12\mu}$ is often used to estimate the cloud phase by simple thresholding method:

cloud phase	$T_{12\mu}$
water	$T_{12\mu} > T_{th}$
ice	$T_{12\mu} < T_{th}$

with a threshold value of about $T_{th} \approx 260K$. In this case, the thermal radiance in the window channel must be an additional input in the cloud analysis subsystem.

6.5.3 SEVIRI case

Ratio of the reflectance at 1.6μ and 0.65μ or 0.85μ allows phase determination using a threshold value of 0.45 (TBC) (see [Jo99]) :

cloud phase	$\frac{\rho_{1.6\mu}}{\rho_{0.85\mu}}$
water	> 0.45
ice	< 0.45

6.5.4 Validation

Phase determination using visible band imager channels will be validated using ATSR-2 data. For Meteosat-7 this validation must be done.

6.6 Cloud Coverage - TBD

6.6.1 Introduction

The cloud coverage subsystem aims to discriminate between spatially homogeneous cloud layer (stratiform) and "broken" cloud (cumuliform). This discrimination is not possible in a single imager pixel and could only be derived at lower resolution.

In the RMIB GERB processing, cloud coverage is estimated on areas including 3*3 imager pixels. The cloud coverage product has then a spatial resolution reduced by a factor 3. The 3*3 pixel windows correspond to approximate footprint size of 10*10 km.

6.6.2 Meteosat-7 case

TBD

6.6.3 SEVIRI case

TBD

6.7 Cloud Shadow

6.7.1 Introduction

At dawn and dusk, cloud shadow can be observed along the (high level) cloud borders. In shadowed areas, the derived cloud optical thickness may become negative because the current reflectance ρ may be under the clear sky reflectance ρ_{cs}. Cloud analysis contains a separated cloud shadow flag product.

6.7.2 Implementation

The shadow flag is set for pixel with

$$\rho < 0.9\,(\rho_{cs} - 0.05)$$

6.8 Fresh Snow Flag - TBD

Method to discriminate between fresh snow (which does not on the clear sky images because of the inertia of the clear sky building process) and cloud should be developed and implemented.

6.9 Implementation

The cloud analysis is perform by the RMIB program 'cloudanalysis'. Except for development, the cloud analysis is not split into separated small programs because in this case a lot of time will be spend for data input/output on disk. It should be recall here that the cloud analysis should be done within 15 minutes to reach real-time analysis of the SEVIRI slots.

The cloud analysis subsystem takes as input :

- the reflectance image(s) for the current slot,
- the clear sky reflectance image(s) for this slot,
- the images of viewing angles geometry (θ_s, θ_v, ϕ) valid for the current slot,
- the table(s) of overcast scene NB reflectance $\rho_{over}(\theta_s, \theta_v, \phi)$: one table for MS7 but three table for SEVIRI.

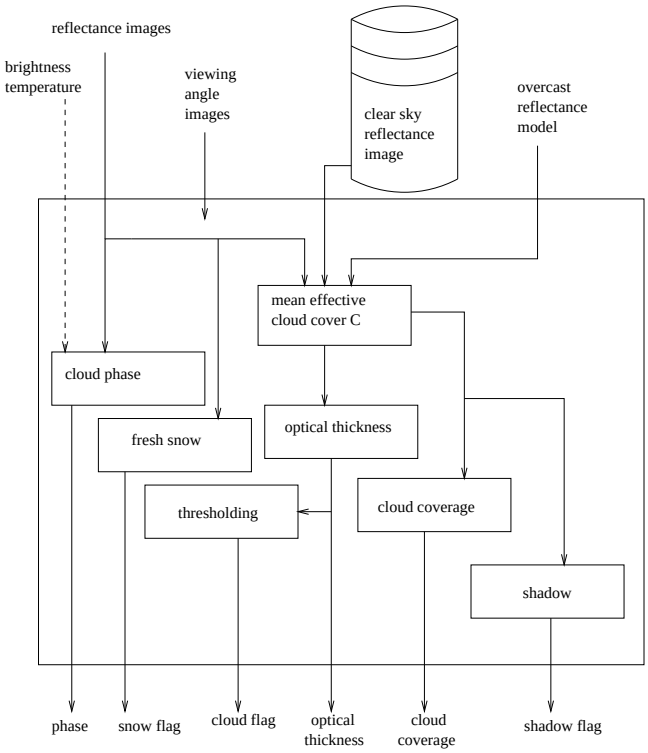

Figure 9: Overview of the cloud analysis subsystem within the scene identification system of the RMIB GERB Ground Segment.

- The brightness temperature image T_B (for Meteosat-7 only).
- the surface identification results at high and middle resolution

and generates the following list of products :

- the cloud flag image (see 6.4),
- the cloud optical thickness image (see 6.3),
- the cloud phase image (see 6.5),
- the shadow flag image (see 6.7),
- the fresh snow flag image (see 6.8),
- the cloud coverage image (see 6.6),

All products are derived at high and mid-resolution, excepted the cloud coverage image which could only be derived at mid-resolution.

7 Conclusions

This document describes the scene identification subsystem of the RMIB GERB processing. The scene identification system does not aim to select the most appropriated angular dependency model for each pixel in the imager FOV but aims to deliver intermediate products (in the form of images) that serve as basic inputs for the choice of ADM in a separated subsystem (described in [AD8]). This separation allows the development of a scene identification which is not dependent on the set of ADM that are available.

References

[NC01] "Generation of a Data Set of Earth's Scenes Spectral Signature", RMIB GERB Ground Segment internal documentation, Nicolas Clerbaux, June 1999.

[SSP] "SEVIRI Science Plan", Version1, 27 march 1998, EUMETSAT (available for down load from EUMETSAT web site, http://www.eumetsat.de/publication)

[PINT] "The integral program', BATS library documentation, 1999.

[MA79] "Multivariate Analysis", K.V.Mardia, J.T.Kent and J.M.Bibby, 1979, Academic Press.

[PLMS] "Least Square User's Manual", BATS library documentation, 1999.

[FILT] "Spectral Response Curves used at RMIB for the GERB Ground Segment", GERB Ground Segment documentation, Nicolas Clerbaux 1999.

[SBDART] "Santa Barbara Disort Atmospheric Radiative Transfer : A Practical Tool for Plane-Parallel Radiative Transfer in the Earth's Atmosphere", P. Ricchiazzi, S. Yang and C. Gautier, Earth Space Research Group, Institute for Computational Earth System Science, University of California, Santa Barbara. Available from web site : http://arm.mrcsb.com/sbdart.

[OT97] "Modeling Zenith-Angle Dependence of Outgoing Longwave Radiation : Implication for Flux Measurements", J. Otterman and al. , REMOTE SENS. ENVIRON. 62:90100, 1997.

[ERB] "Angular Radiation Models for the Earth-Atmosphere System", Volume 1 : Short wave Radiation, J.T. Suttles and al., July 1988, NASA Reference Publication 1184.

[AD5] "RMIB GERB Processing : Spectral Modeling", RMIB documentation,1999.

[AD7] "RMIB GERB Processing : Scene Identification", RMIB documentation,1999

[AD8] "RMIB GERB Processing : Angular Dependency Models", RMIB documentation,1999.

[Jo99] "Requirements for the synergetic use of the ERM imager", Deliverable for ERM passive instrument synergy study, KNMI, Jolivet, 1999.

[De99] "The need of Angular Dependency Models for the Geostationary Earth Radiation Budget short wave flux estimation", S. Dewitte and N. Clerbaux, proceedings of the ALPS99 conference, CNES, January 1999.

[De98] "Exploitation of GERB for climate and meteorological applications - WP2000: Detailed analysis of user needs", S. Dewitte, RMIB, Sept. 18^{th} 1998.

[SR91] "Solar Radiation Atlas of Africa", E.Raschke and R. Stuhlmann, Published for the CEC, 1991.